6. Tropospheric Pollution

Air pollution resulting from human activities is causing increasingly diverse health problems and affecting larger and larger areas. Smog, ozone, and particulates affect our lungs and eyes. Mercury from fossil fuel burning is being spread everywhere, like the proverbial pink goo in Dr. Suess' *The Cat in the Hat Comes Back*. Acid rain resulting from fossil fuel burning diminishes habitat and encroaches on biodiversity. Sulfate aerosol from fossil fuel burning also exerts a strong influence on the heat budget of the earth, since they reflect sunlight, partially offsetting the greenhouse warming effect of increased CO_2 emissions.

Burning fossil fuels and vegetation emit a rich suite of chemical compounds which are precursors to the formation of tropospheric ozone. With more people burning tropical jungle material we are seeing increasingly large palls of smoke covering larger areas of the tropics. The chemicals that are produced then "cook" in the sunlight, creating high concentrations of ozone. In September over the tropical South Atlantic ozone concentrations reach over 100 ppbv, similar to a polluted summer day in Atlanta. While this is perhaps shocking due to the remoteness from population centers, a much more widespread problem is the strong tropospheric ozone pollution which occurs every northern summer over most of the northern hemisphere, the accumulated output of megacities such as Beijing and Mexico City (Fig. 6.1). Sub-continental scale pollution can be seen in northern India in Fig. 6.2. Continental-scale pollution is blown across the oceans to the next continent. This northern midlatitude westerly merry-go-round of chemical compounds has gained the concern and attention of the global community. A focus on the TRACE-P mission helps illuminate the need for international cooperation in dealing with air pollution.

Figure 6.1. Air pollution in a) Beijing China during March 2009 and over b) Mexico City during March 2006.

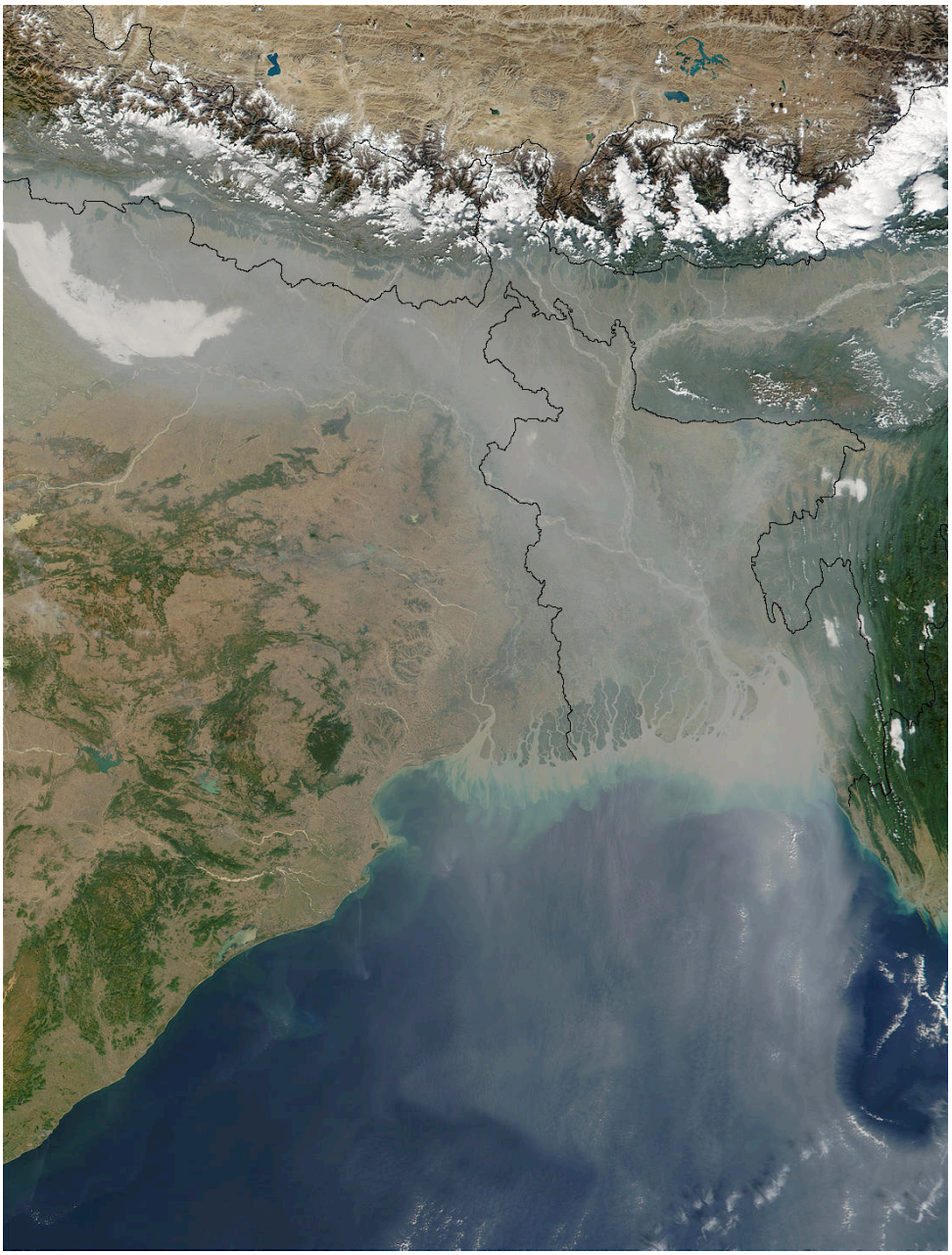

Figure 6.2. MODIS image of Northeastern India, Bangla Desh, and the Himalayas in November 2001 showing a large region of polluted air streaming offshore into the Bay of Bengal [http://www.ssec.wisc.edu].

6.1. Burning Fossil Fuels

When fossil fuels and vegetation are burned, oxygen combines with trace amounts of sulfur in the fuel to create "odd sulfur" gases $SO_x = SO + SO_2$, called "sox", while oxygen combining with nitrogen from the air at high temperatures creates "odd nitrogen" gases $NO_x = NO + NO_2$, called "nox". In addition, trace amounts of mercury in the fuel and a wide range of particulates and volatile organics are emitted. When sufficiently intense sunlight shines on this mixture, ozone can be created in the troposphere. Taken together, all of these emissions

negatively impact human health. Fine particle concentration is correlated with mortality rate. Tropospheric ozone is correlated with lung and eye problems and probably kills more people than the increased skin cancer deaths resulting from reduced stratospheric ozone.

Current Environmental Protection Agency (EPA) standards declare 188 toxic pollutants, including Hg and VOCs to be dangerous at any level. An EPA "bright line" value for health alerts determines the legal threshold for exceeding recommended health guidelines. Some individuals will be affected at lower levels and there will be a range of responses among individuals. PM2.5 is a measure of the mass of particles, solid and liquid, of a radius less than 2.5 μm, which are especially dangerous because they can more readily reach the distributed recesses of the alveoli in our lungs. PM10 includes windblown dust, which is not generally as harmful as the smaller particles. The PM2.5 "bright line" value of 35 $\mu g\ m^{-3}$ is the current value for an EPA health alert, reduced from 65 $\mu g\ m^{-3}$ prior to October 2006. Yet the strong correlation between PM2.5 exposure and negative health consequences extends to well below 35 $\mu g\ m^{-3}$.

The EPA bright line for ozone is 80 ppbv, but Canada and Japan set their health alert thresholds at 60 ppbv and the EPA is considering resetting the bright line for ozone to 60 ppbv. There is no abrupt change in health risk above and below a bright line. It is a continuum of risk. Since the 1990 Clean Air Act it has cost the utility industry about 800 million/yr (0.6 % of total operating costs) but has saved much more per year in terms of reduced health care costs, and reduced degradation of ecosystems and human constructions.

The U.S. emits more than 100 tons of Hg, 40% in power plants and 60% by vehicles burning fossil fuels. This toxic metal builds up in aquatic predatory fish and causes irreversible nerve damage. It is especially dangerous for pregnant women and children to consume fish from lakes with significant Hg. It is estimated that more than 600,000 babies are born each year in the U.S. with noticeable effects of Hg poisoning (Johnson 2005). Although many states have tried to enforce their own guidelines for Hg emission from coal burning power plants, the EPA has mandated more modest reductions over a longer period. For the first time, the EPA has issued controls on the emission of Hg from from coal-fired power plants, to begin in November 2011.

The economic attribution for sources of these pollutants is broadly distributed across a wide array of economic subdivisions: electric utilities, transportation, industrial combustion, and residential combustion. Every family is responsible for generating some of the pollutants. Considering that it takes 1 lb of coal to create 1 kW-hr of electricity and that the average U.S. family uses about 10,000 kW-hr of electricity each year, then each family uses 10,000 lb of coal per year for generating electricity. This pervasive and diverse array of usages makes the problem of reducing the 30 million metric tons of emission for each of SO_x, NO_x, and volatile organics particularly hard to solve.

6.2. Tropospheric Ozone Chemistry

Tropospheric ozone directly harms eyes and lungs and, with acid rain, is devastating to plants. It also absorbs infrared near 9.6 μm and is therefore a moderately important greenhouse gas. Ozone and OH are the major oxidants of N, S, CO, and hydrocarbons, which would otherwise build up in the atmosphere. Brasseur et al. (1999) estimated that, collectively, about 20×10^{28} ozone molecules per s enter the troposphere from the stratosphere in tropopause folds near midlatitude cyclones. This roughly balances ozone loss in the oceanic boundary layer. Sunny industrial boundary layers produce about 8×10^{28} ozone molecules per s, roughly

equalling ozone destruction in the free troposphere. It remains a challenge to quantify how much ozone is produced locally, how much is produced far away, and how much comes from the stratosphere.

Tropospheric ozone maximizes near populated land masses in northern summer. Since 1900 the amount of tropospheric ozone has approximately doubled, but high amounts are concentrated in specific regions. This has been compensated by stratospheric ozone loss due to CFCs over the past 20 years. Since tropospheric ozone molecules are closer to the surface they exert a stronger greenhouse gas influence on surface temperature than do stratospheric ozone molecules.

A chemical pathway for the production of significant amounts of tropospheric ozone was first described by Crutzen (1973) and Chameides and Walker (1973). The conceptual challenge was that most of the xuv photons needed to make atomic oxygen are absorbed in the upper atmosphere. Since there aren't enough xuv photons to break apart O_2 in the troposphere, O_3 must be produced by a fairly complex process involving NO_x plus a heady mixture of CH_4, CO, and a wide variety of non-methane hydrocarbons (NMHCs) such as pinene, plus uv photons that reaches the surface on a sunny day. While the photochemistry is very complex, the following relation captures some of the primary aspects of ozone smog chemistry:

$$NO_x + \{CH_4 + CO + NMHCs\} + uv \rightarrow 0_3 + \text{aldehydes} + PAN \qquad (6.1)$$

The limiting constituent is usually NO_x. It acts as a catalyst, consuming NMHCs. In general, if more NMHCs or more NO_x is added, the more ozone can be made.

Figure 6.3 describes the diurnal cycle in polluted cities, with morning commuters emitting NO_x and HC. This leads to the production of aldehydes and ozone in the afternoon. Note also the formation of PAN, peroxyacetyl nitrate, a long-lived nitrogen compound that can be transported far from its source and participate in pollution chemistry somewhere else far downwind.

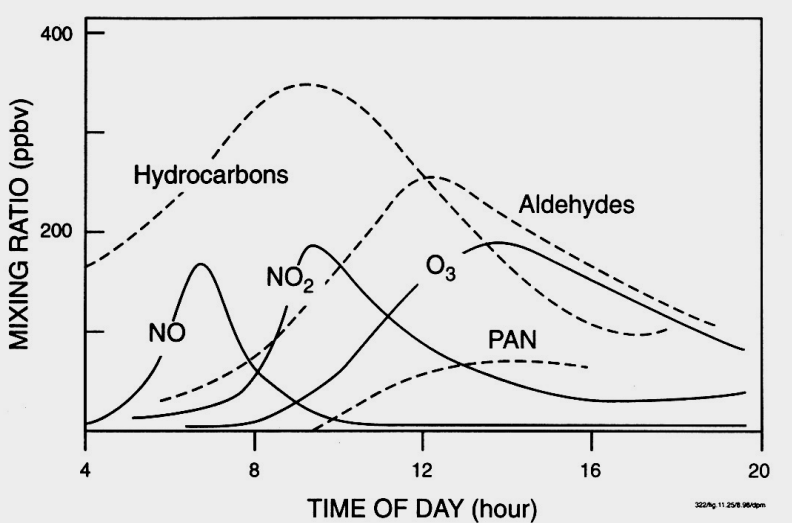

Figure 6.3. Evolution of the chemical composition of the lower atmosphere during a smog event (Goody, 1995).

The seasonal distribution of tropospheric column ozone is shown in Fig. 6.4 (Fishman et al., 1990). This tropospheric ozone residual was obtained by estimating the stratospheric contribution to column ozone from the SBUV instruments, and subtracting that from the total column obtained by TOMS. Although the largest ozone pollution signal is clearly in the NH spring and summer (middle panels), a big surprise lay in the middle of the South Atlantic between Africa and South America during NH fall. Ozone can readily exceed EPA thresholds while sailing in a boat in the middle of the Atlantic, far from any combustion source! How can this be? It was determined that the influx of people into the jungles of Amazonia and Africa led to a rapid increase in seasonal burning to clear land for planting crops.

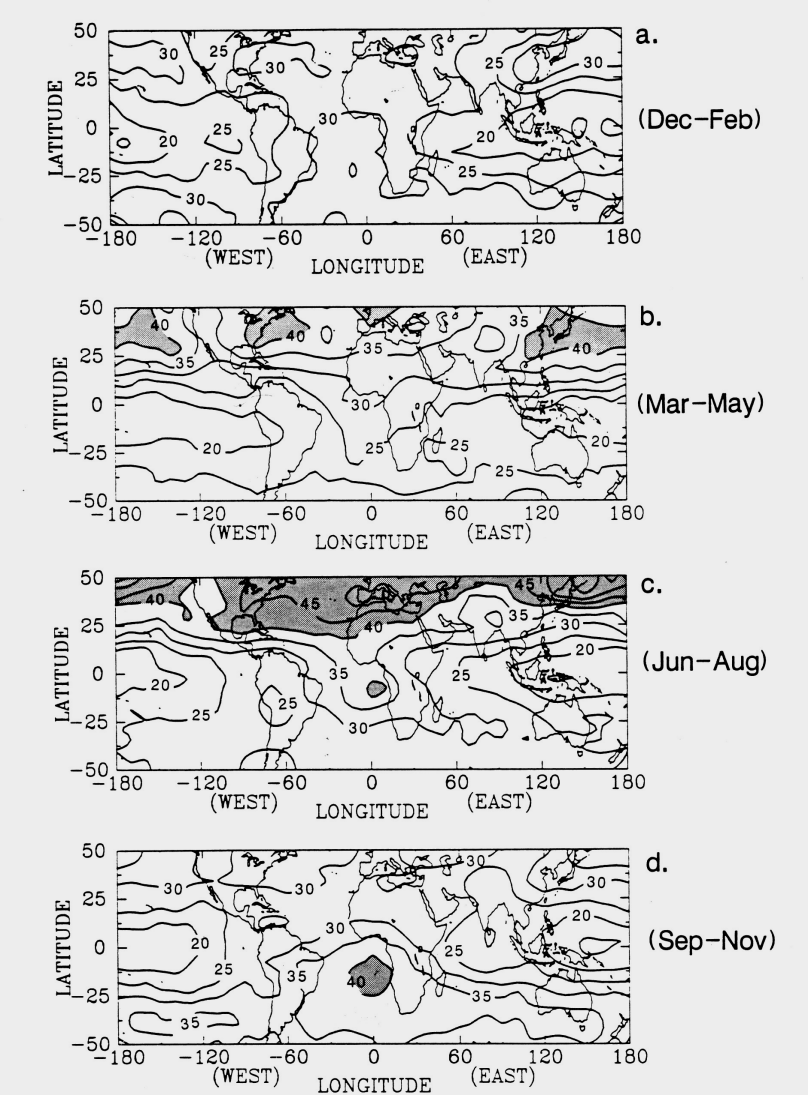

Figure 6.4. Seasonal mean distributions of tropospheric column ozone for NH a) winter, b) spring, c) summer, and d) fall, contour interval 5 DU. Amounts exceeding 40 DU are shaded. (From Fishman, et al. 1990).

Figure 6.5 shows the change in seasonal biomass burning from 1973 to 1988 in Amazonia. This rich mixture, as potent as any in Los Angeles, is transported upward in thunderstorms, spread out over the Atlantic Ocean, where it subsides in the subtropical Atlantic high pressure system and cooks in the hot sun.

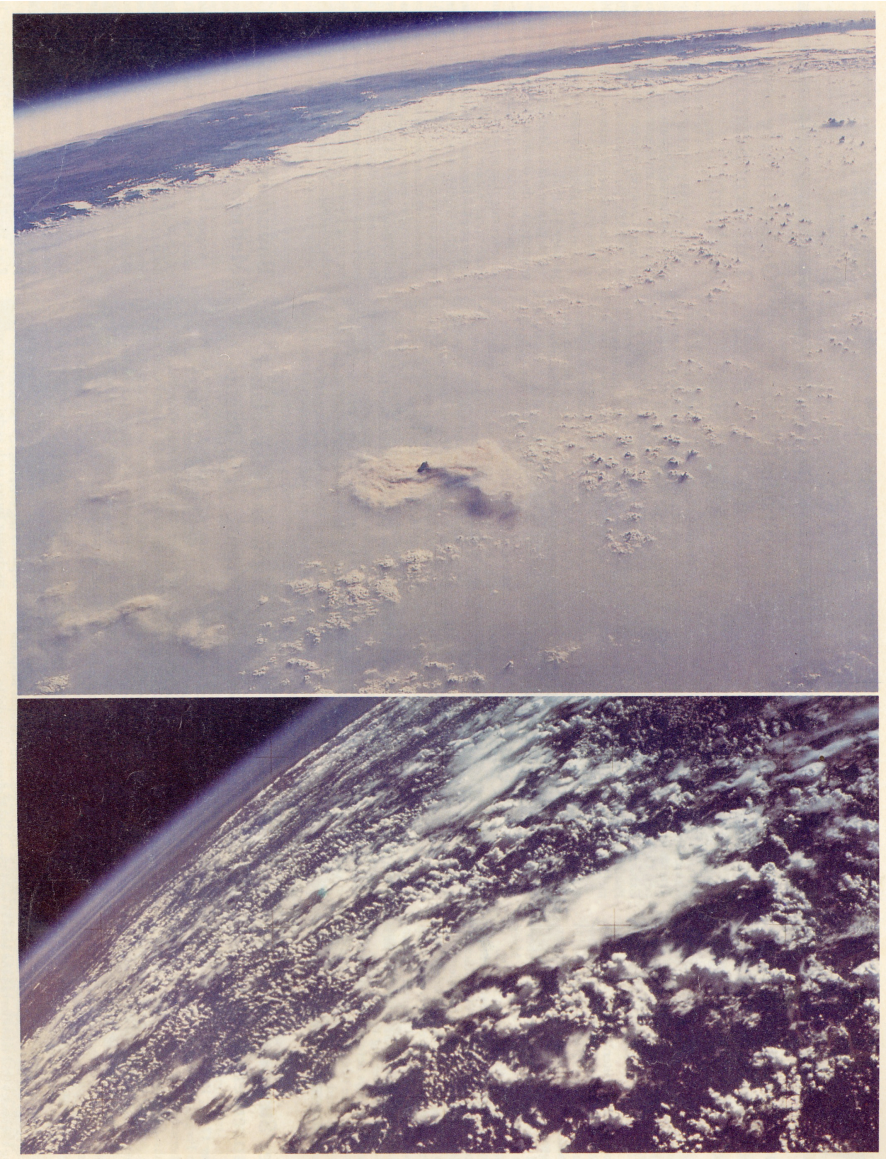

Figure 6.5. Space shuttle photographs of Amazonia during the September biomass burning season showing the marked increase from 1973 to 1988.

Figure 6.6 shows the seasonal change in African fires which contribute to this subtropical South Atlantic pollution problem. During August fires are set to clear brush in subtropical South Africa, adjacent to the South Atlantic anticyclone, where high concentrations of ozone are found (Fig. 6.4d).

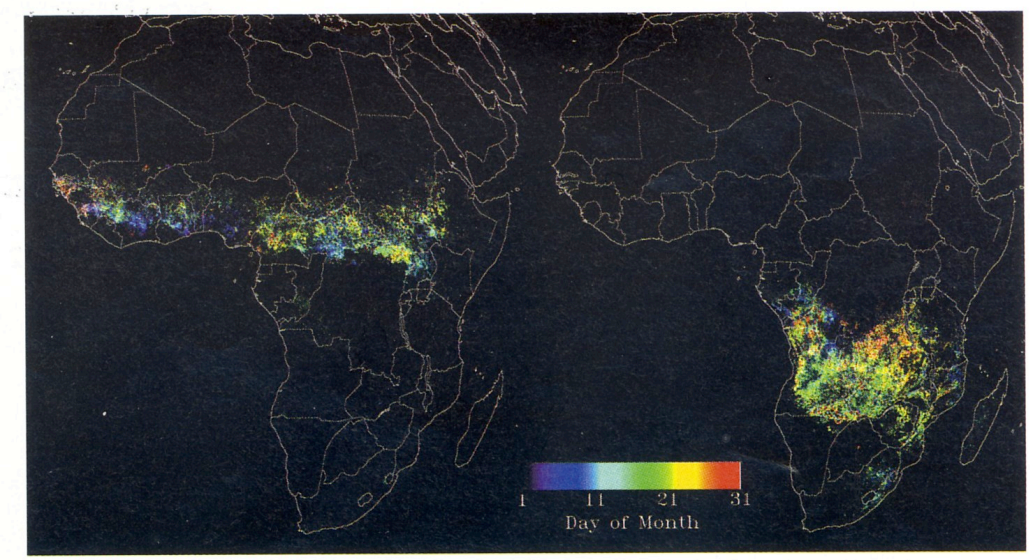

Figure 6.6. Fires detected by SEVIRI for (left) February and (right) August 2004 (Roberts and Wooster, 2007).

Returning to Fig. 6.4, In NH spring one may observe high ozone amounts on the east coasts of North America and Asia. In March the sun is shining more strongly on midlatitude urban centers, making more ozone (see Fig. 6.1). Also, there are climatological troughs in these longitudes, preferred regions for the entry of stratospheric ozone into the troposphere. Quantification of the relative amounts of ozone from pollution and from the stratosphere over East Asia was a primary goal of the TRACE-P experiment.

NH summer is characterized by elevated ozone amounts throughout the entire extratropical hemisphere. Some regions with chronic high pressure with stagnated air are particularly susceptible to ozone pollution, such as the southeastern U.S. (Fig. 6.7). Ozone forecast models generally do a good job of anticipating these events, which can help save lives. These models are also useful for estimating the benefits of reducing NO_x or NMHCs. NO_x reduction exerts a much stronger effect on ozone mitigation, but in strongly polluted cities, NO_x reduction can lead to an increase in ozone (Brasseur et al., 1999).

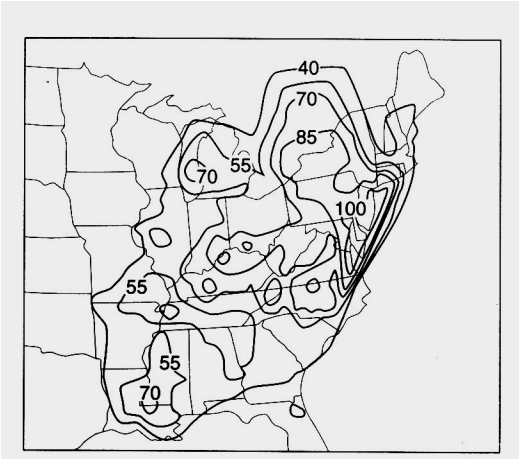

Figure 6.7. Ozone mixing ratio (ppbv) observed during a pollution event in the summer of 1986 by the EPA ozone monitoring network (Fehsenfeld and Liu 1993).

6.3. Sulfate Aerosol

Volcanoes have belched forth sulfurous fumes since the world began. Much of it has been incorporated into rocks. The sulfur that is in the earth system is cycled among the different spheres. Phytoplankton produce a fair bit of sulfur compounds, primarily dimethyl sulfide, $(CH_3)_2S$), and carbonyl sulfide (COS), which can lead to SO_2 formation. Volcanoes also lead to SO_2 production. But with the rise of the industrial age, anthropogenic sulfur emissions surpassed natural sources four-score years ago. Today fossil fuel burning contributes about four times the emission from natural sources. Humans are altering the global sulfur budget to a considerable degree. Annual U.S. emissions of S grew from 5 Tg/yr in 1900 to 15 Tg/yr in 1970, with a decline to 12 Tg/yr after the U.S. Clean Air Act of 1970. Annual U.S. emissions of N grew from 1 Tg/yr in 1900 to 5 Tg/yr in 1970, and leveled off thereafter. Global emissions, however, have continued to grow, reaching 80 Tg S/yr and 30 Tg N/yr.

Fossil fuel burning and biomass burning emit SO_2 and NO_2, which combine with OH molecules to make sulfuric acid, H_2SO_4, and nitric acid, HNO_3, within a few hours. Sulfuric acid can condense with water vapor into droplets of sulfuric acid trihydrate, ($3\ H_2O \cdot H_2SO_4$), with sizes typically 0.1-1.0 μm. A haze of these droplets can reflect sunlight, absorb sunlight, absorb infrared, and reduce visibility. Sulfuric acid and nitric acid can get incorporated into hydrometeors and fall to the surface, removing the pollution from the atmosphere. The hydroxyl radical acts as a tropospheric cleanser, but acid rain represents a source of acidity to oceans, lakes, rivers, forests, crops, yards, and buildings. If it takes 5 days from point source emissions to acid rainout, and if the average wind speed in midlatitudes is assumed to be 5 m/s, then acid rain will be spread at least 2000 km downwind.

Sulfate droplets and other anthropogenic aerosols add to the ambient natural droplet nuclei. This spreads any condensing gaseous water vapor over many smaller droplets. The average droplet radius is much smaller near industrialized regions. As a result, clouds may last longer and precipitation may be delayed. This is referred to as an aerosol indirect effect on the radiation budget.

By absorbing and emitting infrared, sulfate aerosol keeps the nighttime warmer than it would be without them. By reflecting sunlight during the day, sulfate keep the daytime cooler than it would be without them. The day/night temperature range, or *diurnal range*, has decreased by more than 1 K in the last century, consistent with this interpretation. In major fossil fuel burning regions, radiative observations and calculations show that anthropogenic aerosol reflects 2-10 W m^{-2} of solar energy back to space across North America and Eurasia. Figure 6.8 shows the regional cooling effect of anthropogenic aerosol resulting from burning. Both the midlatitude fossil fuel burning sources and the tropical biomass burning sources are evident.

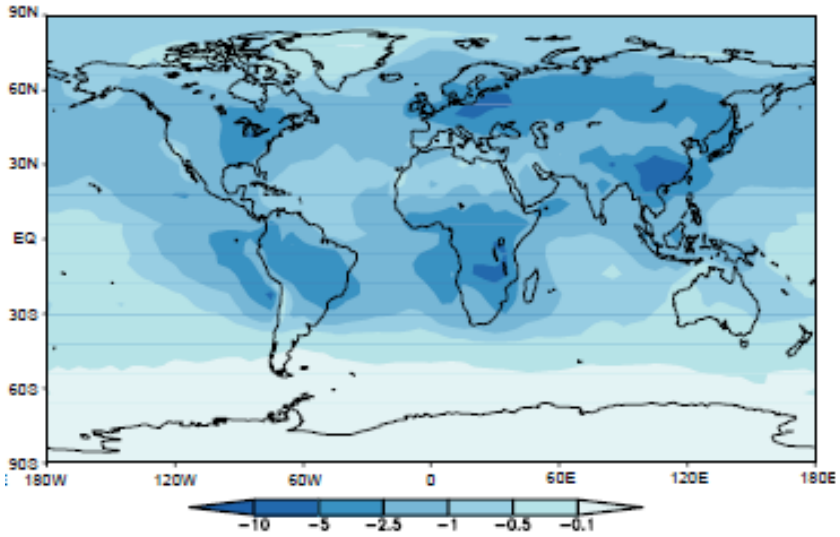

Figure 6.8. Annual mean anthropogenic aerosol forcing in W m^{-2} (Chen and Penner 2005). Larger negative values (darker blue) correspond to more solar radiation scattered back to space.

The radiative effects of aerosol are compared with CO_2 increases and other factors in Fig. 2.10. Long-lived greenhouse gases have contributed an extra 2.7 W/m^2 radiative forcing at the surface since 1750. Increases in tropospheric ozone have added 0.3 W/m^2 in the 9.6 μm band, while reductions in stratospheric ozone reduce this slightly. The rise in CH_4 has led to more H_2O in the stratosphere, which emits a little more infrared to the surface. Changes in surface albedo include increased reflection from cities and roads but increasingly widespread sooty snow enhances absorption of sunlight and fosters melting. Note the large uncertainties in the effects of aerosol. The direct effect of reflecting sunlight is -0.5 W/m^2, but with large uncertainty. Changes in the composition and distribution of aerosol are uncertain. The indirect effect of making clouds last longer and reflecting more sunlight is -0.7 W/m^2, with an even larger uncertainty (Fig. 2.10). The solar reflecting quality of anthropogenic aerosols significantly offsets increased downwelling infrared emission by greenhouse gases, with a net effect of 1.6 W/m^2. To emphasize the uncertainty, especially the spatial variability of the effects of sulfate aerosol, it should be noted that many surface observations of solar radiation showed a reduction of 20 W/m^2 over the period 1958-1985. This global dimming appears to have slowed or reversed since then.

The production of DMS by oceanic phytoplankton greatly interested James Lovelock, who hypothesized that they had a planetary thermoregulatory capability. In the natural world over the oceans there are relatively few cloud condensation nuclei (CCN). DMS emitted by phytoplankton in sunlight can create effective CCN and form clouds. If there is too much sunlight and CCN clouds will shut off the sunlight and DMS formation so that clouds will go away and the sun will come out again. This biologically-mediated stable feedback cycle is sketched in Fig. 6.9. By regulating cloudiness and sunlight, phytoplankton help keep the planet's temperature near an equilibrium. Thus, any climate perturbation would be resisted by the mechanism shown in Fig. 6.9, tending to restore the status quo. This is an example of the Gaia hypothesis in that the earth's biosphere helps regulate the climate of the earth. We will return to this theme and that of competition and cooperation in discussing Daisy World in Chapter 10.

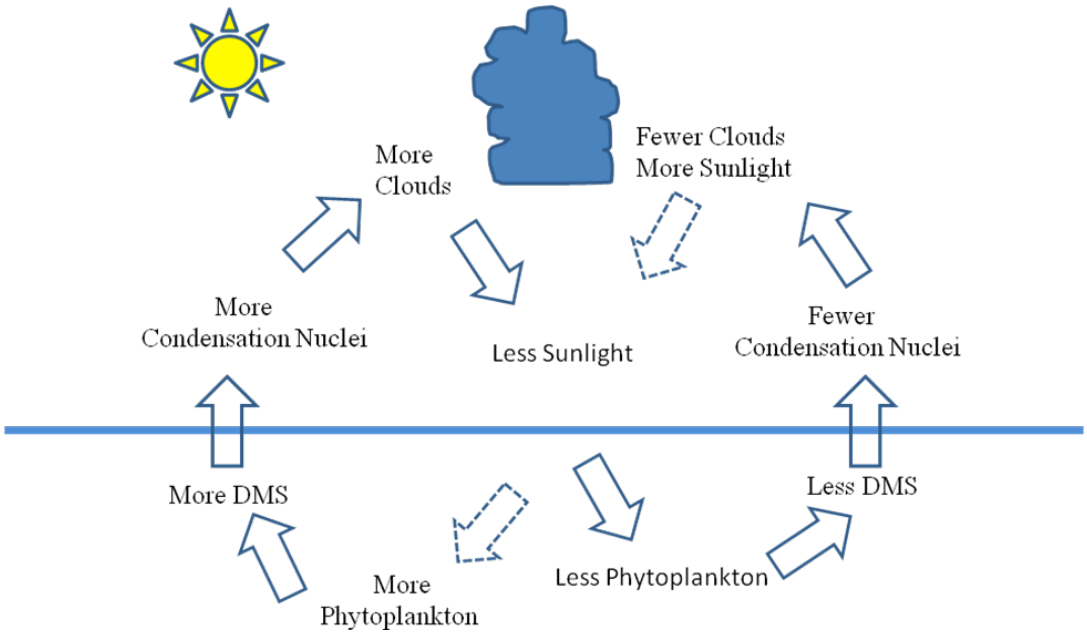

Figure 6.9. Schematic diagram of James Lovelock's hypothesis that ocean phytoplankton may help thermoregulate the planet by producing DMS, which forms cloud condensation nuclei. The natural system is an infinite stability cycle: more phytoplankton create more clouds, which shut off sunlight, so less DMS is produced, so clouds dissipate, letting in sunlight, producing more phytoplankton, more DMS, and more clouds.

6.4. Acid precipitation

The acidity of sulfate aerosol, rain, or snow is measured on the pH scale, named after the *p*ower of the *H*ydrogen ion. Clean water has 10^{-7} moles l^{-1} of hydrogen ions, H^+. The pH is defined to be $-\log_{10}[H^+]$, which is 7.0 for clean water. With increased concentration of $[H^+]$ there is a smaller negative power in moles l^{-1}, so the pH gets smaller, and the precipitation is more acidic. Battery acid has a pH of 1, lemon juice 2, coca-cola 4, natural rain water 5.6, and sea water 8.0. With decreased concentration of $[H^+]$ there is a larger negative power, so the pH is larger, and it is more basic. Calcium carbonate ("lime") has a pH of 8.2, making it useful for reducing the acidity of an ecosystem. Ammonia has a pH of 11, and bleach has a pH of 12.

Why is the pH of rainwater less than pure water? Natural rainwater has dissolved CO_2 in it, in the form of carbonic acid, H_2CO_3:

$$H_2O\ (\text{liquid}) + CO_2\ (\text{gas}) \rightarrow H_2CO_3\ (\text{aqueous}) \qquad (6.2)$$

This removes some CO_2 from the air and slightly acidifies typical rainfall. With the rise of atmospheric CO_2, more is dissolving in the ocean, making it more acidic. This is of tremendous concern since the pH controls the distribution of fundamental primary producer ecosystems by controlling where calcium carbonate will dissolve into solution. If primary productivity in the ocean declined due to acidity, it would make the ocean less able to take CO_2 out of the atmosphere.

Acid fogs with a pH of 1.5 have been observed in Los Angeles. A visit to my grandmother's house each summer in the 1960s brought headaches and a tight neck every time. But Los Angeles was not the first place to be plagued with smog. A great deal can be learned about conditions in England from John Evelyn's 1661 treatise "Fumifugium, or the Inconvenience of the Aer and Smoak of London Dissipated". By 1000 A.D. much of the forests of England had been cut down, but an abundant soft coal, called sea coal, was available from the northeast coast. It was plentiful, cheap, but rather inefficient. People complained about the noxious smoke it made and in 1272 King Edward banned the use of sea coal. But the problem worsened over the centuries. Evelyn waxed indignant about the smoke's effects in London and successfully campaigned to move all coal burning industries out of the city toward the mouth of the Thames. This helped, but by 1800 there were more than 1 million people living in London, all relying on coal as fuel. One episode of smoke-fog mixture, or smog, lasted from November to March 1879. In 1952, there was a notably bad smog episode from December 5 - 9, with visibility less than 10 m at Heathrow airport, and the normal daily death rate tripled in London.

The distribution of acidified precipitation in the U.S. and Europe is shown in Fig. 6.10. Specific hot spots are due to a combination of concentrated point source emissions and prevailing westerly wind directions. Since about 1960, precipitation in eastern North America and Europe has had a pH of less than 4.3, between vinegar and coca-cola. In 1988, a tabulation

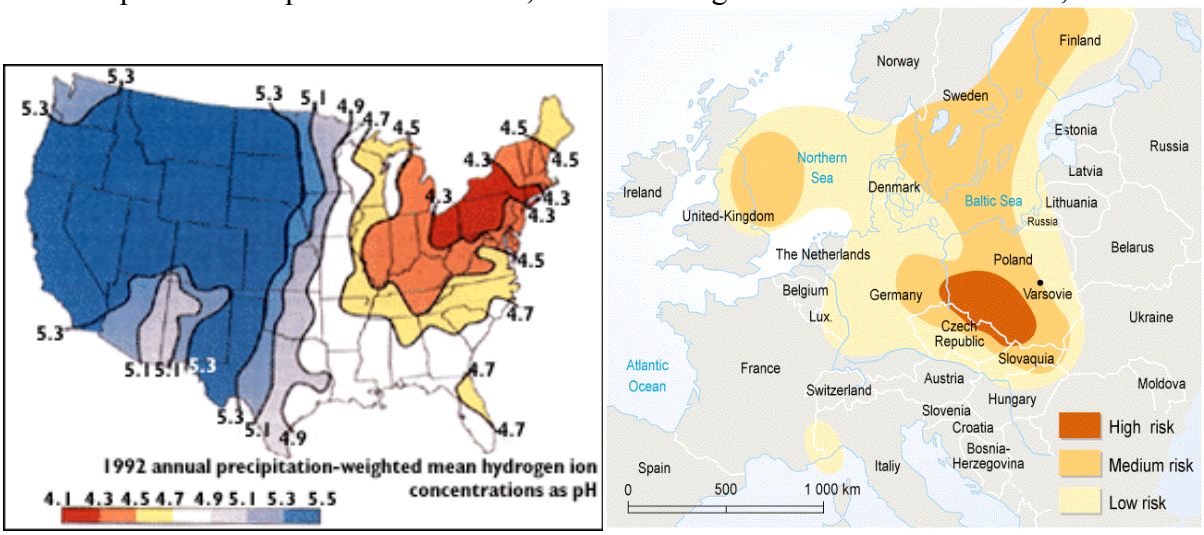

Figure 6.10. Annual mean pH of precipitation in the U.S. during 1992 (left) and risk of ecosystem damage from acid rain in Europe (right).

of estimated acid rain-damaged forest for countries in Europe exceeded 70% in Czechoslovakia, 50% in the United Kingdom, Scandinavia, and Germany, and 30% in most other countries. The exception was Portugal at 20%, which enjoys more pristine westerly winds blowing in from the Atlantic.

Acid rain damages ecosystems by mobilizing toxic metals, interfering with natural metabolic processes of plants and animals, and directly corroding plant tissue and fungi associated with root hairs. Each aquatic species has a different tolerance for acidity (Fig. 6.11). Clams, crayfish, snails, and mayflies are harmed at moderate acidities. Most species fail near a

pH of 5.5. Frogs seem to do okay down to a pH of about 4. In regions where rain and snow have a pH of 4-5, many lakes continue to be stressed. One strategy that has been used successfully in smaller lakes is to reduce the acidity by adding powdered limestone, or calcium carbonate. Having limestone in the subsoil can help buffer the acidity of acid rain. In regions where glaciers scraped limestone away down to Precambrian granite the buffering capability was diminished, leaving central Canada and the Appalachians more susceptible to acid rain.

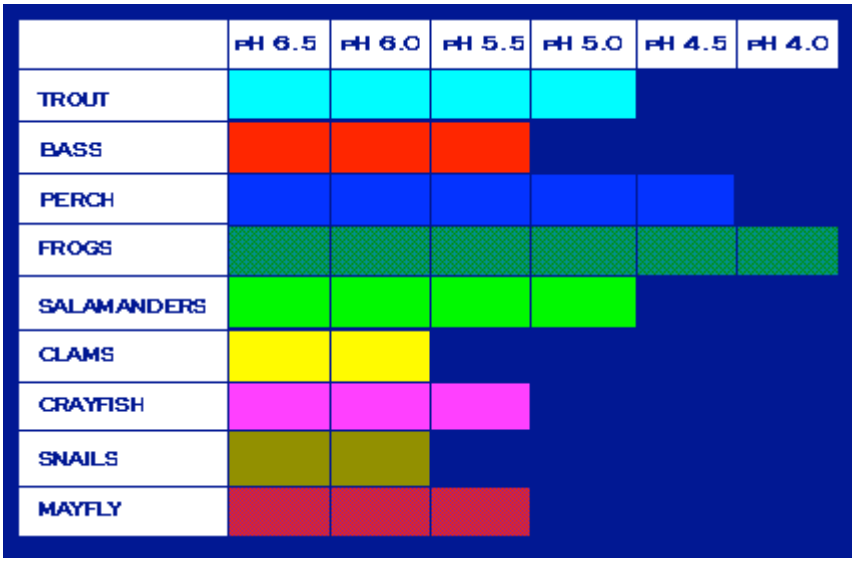

Figure 6.11. Range of pH tolerated by selected aquatic organisms.

Acid rain falling on crops or forests leaches out nutrients, causing a detrimental flow of nitrogen out of forest streams. It mobilizes toxic aluminum in the soil which is taken up by plants in place of the Ca that they need. There is a symbiotic relationship between plants and their mycorrhizae, the thin mycelium of fungi interfacing with the root hairs of the plants. Every tree has its own special mycorrhizal association. If you look around the base of a transplanted tree that has been growing, often in the fall, a "fairy ring" of mushroom fruiting bodies appear in a circle, you can see that each type of tree has a preferred type of associated root fungus. Acid rain kills these fungi, eliminating the capacity for trees to take up essential nutrients. As with the health of coral ecosystems, forest degradation occurs through the influence of several factors, including destruction of the waxy coatings of needles and chlorophyll by ozone. Further evidence that acid rain is hard on symbiotic fungi comes from the general decline of lichens, which are symbiotic fungus-algae combinations, in areas with acid rain. This is too bad, because lichens act to clean the air, feed reindeer, and an infusion in tea may be used to aid lung ailments (Buhner 1996).

It is surprising how pervasive acid rain can be. The prevailing summertime northeasterlies during summer in Hawaii build up stratocumulus clouds against the islands in the elevation range containing a montane forest. But these droplets are often acidified by pollution emitted by cars on the island. In the rainy, pristine Pacific Northwest a similar situation occurs as acidified stratocumulus drench the needles of fir trees in the Cascades. With the introduction of the clean air acts of 1970 and 1991 the acidity of U.S. lakes has eased somewhat and damage to forests has diminished. U.S. sulfur emissions declined by 30% since

1970. Most U.S. monitoring stations are in compliance for being below the standards of 140 ppbv SO_2, 50 ppbv NO_2, and 35 ppbv CO. Yet further progress is clearly needed.

6.5. NASA flight campaign: Pollution from Asia

In the 1990s scientists and policy makers became interested in determining how much of the pollution seen in North America is made there and how much is blown across the Pacific from Asia. NASA aircraft were flown off the east coast of Asia during March-April 2001 to quantify the amount and types of chemical compounds and aerosols coming out of Asia and being transported across the Pacific during the TRansport of Aerosols and Chemicals Experiment in the Pacific (TRACE-P) campaign. Fully instrumented DC8 and P3 aircraft, each measuring over 60 constituents and properties, were deployed from Hong Kong and Yokota air base near Tokyo Japan.

Our role was to forecast meteorological events for flight guidance a day before the flight. Due to computational and time constraints, we were able to run simulations at 50 km resolution. One synoptic transport pathway relevant to this region is the "warm conveyer belt", where moist and polluted boundary layer air moves poleward and rises as a cold front approaches, wrapping cyclonically into the upper troposphere, where it is then blown eastward across the Pacific in strong upper-level westerly winds. A mission science task was to determine the extent of cloud processing of chemical constituents as they travel up through a cloud and become detrained in the upper troposphere. The new MOPPIT instrument was equipped to measure CO from space, so another flight mission goal was to obtain *in situ* aircraft measurements of CO in a cloud-free region for comparison with the new MOPPIT satellite instrument.

One of our forecasts showed a convective complex developing near a low pressure center over the east coast of China and moving eastward in the subtropical westerly jet into the Pacific south of Japan, as seen in the IR image of Fig. 6.12. A warm conveyor belt was present, with southerly winds ingesting warm boundary layer air into the convective complex. This situation provided the perfect opportunity to study the fate of pollutants passing through convective clouds. I was given permission to go on that flight, where we obtained correlative CO measurements, then headed for the convective complex, which by this time was located south of Japan and was in a decay phase. We saw enormous brown sheets of pollution streaming out across the Pacific, with CO_2 values reaching 394 ppmv. In an upward spiral through the clouds one of the instrumentation chemists said over the headphones that "we obtained the chemical signature of hydrometeor processing", so we headed back to Yokota air base.

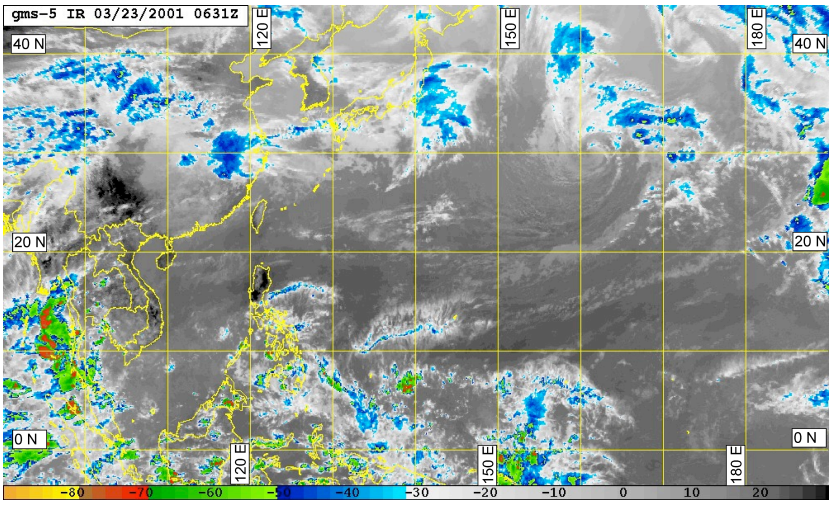

Figure 6.12. Enhance infrared image at 0631 UT March 23, 2001. Note the convective complex over Eastern China that eastward into the Pacific (from Hitchman et al., 2004).

Our forecast mesoscale simulation of this convective complex with the University of Wisconsin Nonhydrostatic Modeling System (UWNMS) is shown in Fig. 6.13. The pink isosurface surrounds the updrafts in the convective complex, which is located above the surface low pressure regions seen obliquely at the bottom. An idealized tracer was initialized in the model to be color-coded red at the surface grading smoothly to blue at the top everywhere in the domain. By 0600 UT March 23 the model had redistributed this tracer, showing the effects of the updraft transporting boundary layer air (red) into the upper troposphere. One may also see evidence of air from the lower stratosphere (blue-green) coming down around the periphery of the thunderstorm into the middle troposphere.

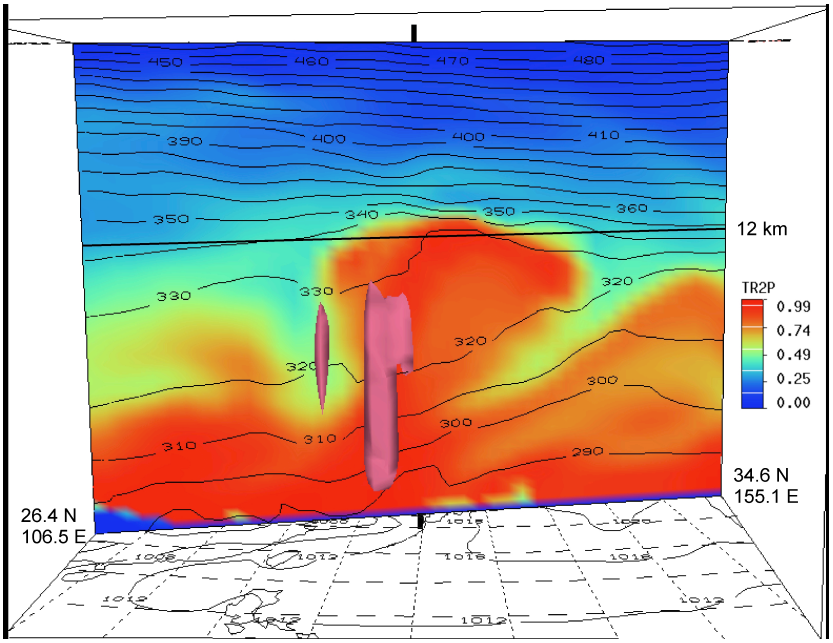

Figure 6.13. UWNMS simulation of the East Asian convective event of March 23, 2001.

Detailed comparison of aircraft observations of ozone and modeled ozone structures confirmed that the circulation near the convection brought low-ozone air (< 40 ppbv) from the oceanic boundary layer into the upper troposphere, while ozone-rich (> 70 ppbv), dry air from the stratosphere was transported down around the periphery of the convection to near 5 km altitude. About 1 Tg ozone (1 Teragram = 10^9 kg) was transported across the tropopause in 24 hours during this convective event. This rate of stratosphere to troposphere exchange is comparable to that associated with tropopause folding in midlatitude cyclones (Hitchman et al., 2004).

One afternoon at Yokota airbase there was animated discussion around some fresh data sheets that scientists had pinned to the hangar walls. It seems that curiously large and irregular spikes of high methane concentrations were occasionally observed in the flight data. Some argued that it was indicative of an upstream source of methane in the jungle of southeast Asia. Others argued that it just had to be from an agricultural source in China. They assumed that the aircraft had flown through sheets of air enriched in methane that had blown out over the Pacific, yielding enhanced values or spikes in the data signal as the instrument sampled the air. All was revealed the next morning, however, when the lieutenant in charge of the hangar and the aircraft stated that henceforth noone would be allowed to flush the forward head (toilet) on the aircraft while the methane instrument was turned on.

6.6. Geophysical box models: Sulfur over the Eastern U.S.

A powerful technique for understanding the roles of different parts of the earth system in determining the distribution of chemical constituents is the geophysical budget approach. The important and complex carbon budget will be discussed in the next Chapter 9. Here a simple budget for sulfur over the eastern U.S. and Atlantic is described as an example (Fig. 6.14). The amount of a constituent in a given *reservoir* is given in kg, while the *flux* of constituent from one reservoir to another is given in kg/s. Atmospheric sulfur is measured in units of 10^9 kg = 10^{12} g = 1 Tg = 10^6 tons = about the mass of a million cars.

Smokestacks and vehicles in the Eastern U.S. emit ~12 Tg S/yr (flux into the atmospheric reservoir), while ~8 Tg S/yr falls back to the ground as acid rain (flux out of the atmospheric reservoir). Since the emission and precipitation of S over land can be estimated fairly well, the geophysical budget approach allows us to infer that ~4 Tg S/yr is transported by winds across the east coast out over the North Atlantic. About 2 Tg S/yr falls into the North Atlantic and ~2 Tg S/yr reaches Europe, where it contributes to their acid rain problem. In comparison, only ~0.2 Tg S/yr is emitted from the ocean surface as a byproduct of phytoplankton metabolism. Humans clearly dominate the sulfur budget of the atmosphere.

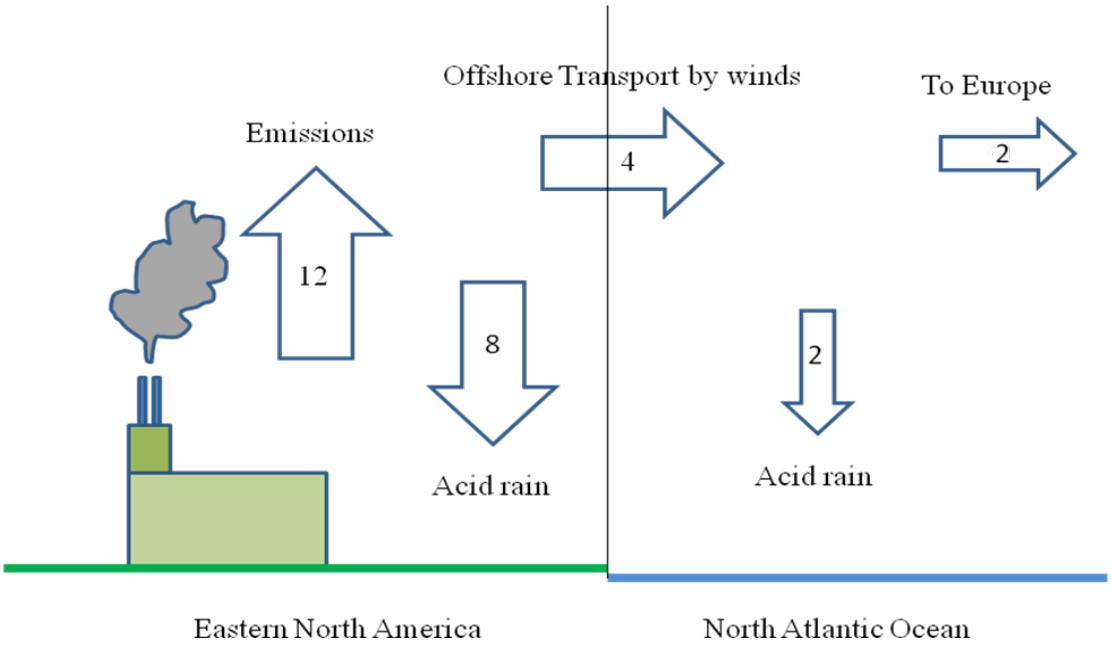

Figure 6.14. Geophysical budget model for sulfur showing fluxes into and out of the atmospheric reservoirs over the Eastern U. S. and the North Atlantic.

6.7. Chemical transport models

The ability of computer models to realistically represent the distribution of chemical trace constituents is growing rapidly. Chemical transport models (CTMs) vary in complexity, with some emphasizing the dynamical details of transport for a single conserved tracer, while others attempt to represent the full photochemistry in as much detail as possible. All efforts are limited by computational resources and the choice in detail of representation depends on the problem at hand. All CTMs make use of the first principles used in weather forecast models. The distribution of model variables such as winds, temperature, pressure, water substance, clouds, and chemical constituents are represented at discrete points in a given volume, the grid points. Differential equations governing the behavior of the atmosphere based on conservation of energy, momentum, and mass for each constituent are applied to the variables, allowing the models to "integrate forward in time" to find the new chemical distributions after each discrete time step. Observations of atmospheric constituents must be initialized. Decisions must be made regarding the treatment of radiative transfer, clouds, and exchange of heat, momentum, and constituents with the surface. The detailed processes that occur in the real atmosphere but lie between model grid points must be "parameterized". An example is treating the complex effects of turbulent mixing by using a simple eddy diffusion coefficient in the model.

To solve for the distribution of tropospheric ozone and other medium-lived pollutants, one needs to know the distribution of temperature and winds, clouds and precipitation, and all of the chemicals that interact with or create the pollutant of interest. The continuity equation governing the concentration, n, of a constituent is given in words as:

Local time rate of change of n = Advection by winds + Production – Loss (6.3)

A photochemical time scale, τ_{phot}, can be defined by dividing the concentration by the loss rate. A dynamical time scale, τ_{dyn}, can be defined by dividing typical distances travelled by typical wind speeds. Constituents with very short photochemical lifetimes have $\tau_{phot} < \tau_{dyn}$ and advection by the winds can be ignored in the "chemical limit" of (6.3). Long-lived constituents have $\tau_{phot} > \tau_{dyn}$ and photochemical production and loss can be ignored in the "dynamics" limit of (6.3).

The characteristic time and space scales of varation of selected trace constituents are shown in Fig. 6.15. Long-lived compounds such as N_2O and CFCs are well-mixed in the atmosphere and spatial variations are only seen at the largest scales (upper right). Short-lived compounds such as the "detergent of the troposphere", the hydroxyl radical, OH, exhibit variations on very small spatial scales (lower left). Compounds such as DMS, SO_2, O_3 and CO have intermediate lifetimes, with interesting spatial variations at regional to continental scale.

To calculate the concentration of ozone accurately one needs to keep track of a range of chemical species that have widely varying time scales. This creates a difficult but interesting challenge for numerical simulations. The time step must be short enough to accurately calculate the short-lived species, but simulations must be carried out long enough to capture the feature of interest, meanwhile keeping track of all of the relevant chemicals and their interactions. This represents a distinct challenge to the computing industry to keep developing faster processors.

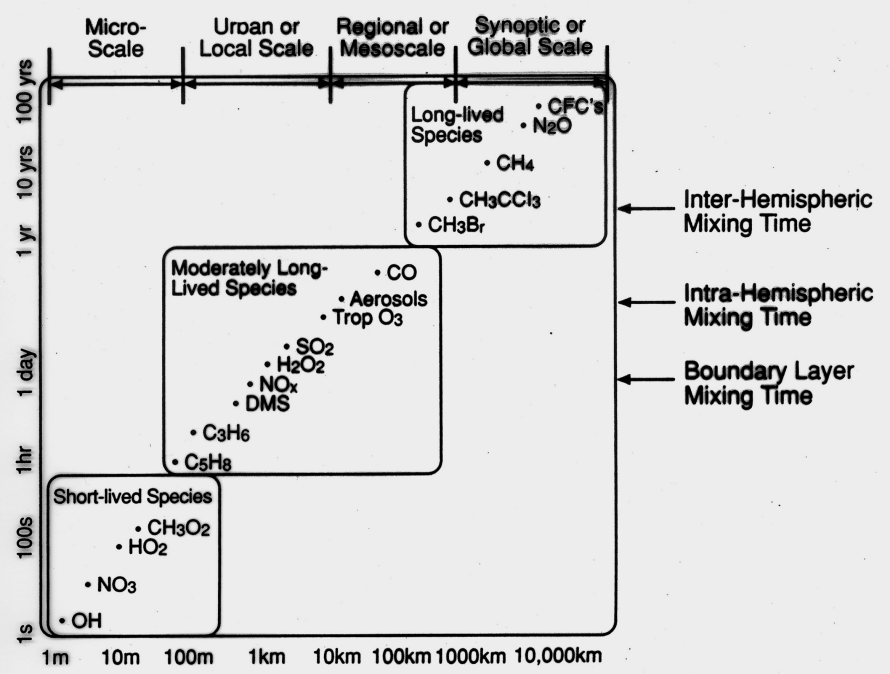

Figure 6.15. Chemical time and space scales (Brasseur et al., 1999).

A model for studying regional air pollution, the CAMx, is available at http://www.camx.org. The EPA and individual states currently maintain a network a network of ozone and PM2.5 monitoring sites which are updated hourly and can be accessed at http://www.airnow.gov. An example of a research model, the RAQMS, that incorporates global

meteorological and chemical distribution information with a detailed photochemistry code, and a local high-resolution model may be found at http://www.raqms.nasa.gov.

CTMs that are coupled with Earth System Models are being used to forecast the future chemical state. One example is the MOZART model, which may be found at http://gctm.acd.ucar.edu/mozart/. The present distribution of ozone during northern summer is compared with the estimated distribution for 2100 AD in Fig. 6.16. Both the NH fossil fuel burning merry-go-round and the tropical biomass burning regimes for tropospheric ozone are expected to increase markedly. Much wider areas of the earth's surface will be exposed to higher levels of ozone. Since ozone damages crops and natural vegetation, increased tropospheric ozone will adversely affect our ability to grow food and for plants to take up CO_2, thereby exacerbating the greenhouse effect.

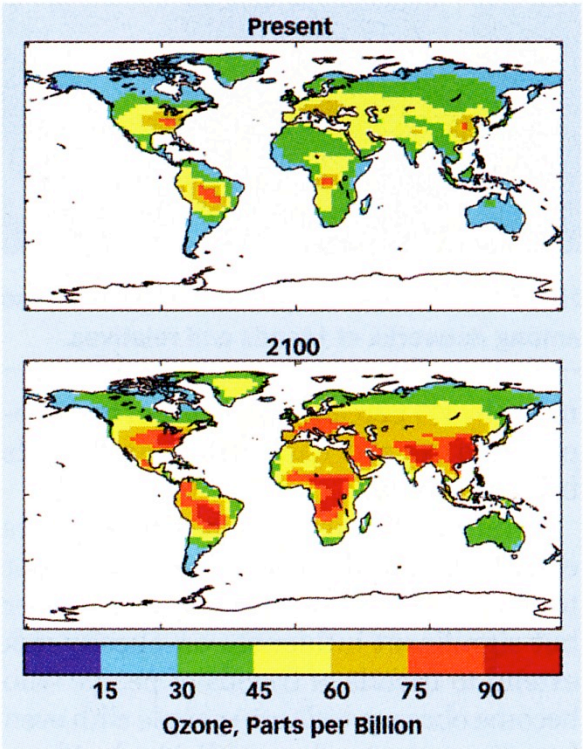

Figure 6.16. Average ozone concentrations during June – August a) today and b) predictions for the year 2100.

Question for discussion. What would happen if we stopped burning fossil fuel and biomass today? Consider both the sulfate cooling effect and the CO_2 warming effect and the removal rates for both constituents. What would happen to daytime maxima, nighttime minima, and to the diurnal range in temperature after we stopped burning?

References Cited

Brasseur, G. P., J. J. Orlando, and G. S. Tyndall Eds., 1999: *Atmospheric Chemistry and Global Change*, Oxford University Press, 688 pp.

Buhner, S. H., 1996: *Sacred Plant Medicine*, *Explorations in the Practice of Indigenous Herbalism*, Roberts Rinehart Publishing, Boulder CO, 210 pp.

Chameides, W. L., and J. C. G. Walker, 1973: A photochemical theory of tropospheric ozone, *J. Geophys. Res*., **78**, 8751-8759.

Chen, Y. and J. E. Penner, 2005: Uncertainty analysis for estimates of the first indirect aerosol effect, *Atmos. Chem. Phys*., **5**, 2935-2948.

Crutzen, P.J., 1973: A discussion of the chemistry of some minor constituents in the stratosphere and troposphere. *Pure App. Geophys*., **106-108**, 1385-1399.

Fehsenfeld, F. C., and **S. C. Liu,** 1991: Tropospheric ozone: Distribution and sources, in global atmospheric chemical change, Ed. W.T. Sturges, Elsevier Applied Science, *London and New York*.

Fishman, J., C.E. Watson, J.C. Larsen, and J.A. Logan, 1990: Distribution of tropospheric ozone determined from satellite data, *J. Geophys. Res.*, **95**, 3599-3617.

Hitchman, M. H., M. L. Buker, G. J. Tripoli, R. B. Pierce, J. A. Al-Saadi, E. V. Browell, and M. A. Avery (2004), A modeling study of an East Asian convective complex during March 2001, *J. Geophys. Res.*, **109**, D15S14.

Goody, R., 1995: *Principles of Atmospheric Physics and Chemistry*, Oxford University Press, 336 pp.

Johnson, J., 2005: "Long Time Cutting", *Chem. Env. Engr.,* Feb. 28, 44-45.

Roberts, G., and M. J. Wooster, 2007: New perspectives on African biomass burning dynamics, *EoS Trans.,* **88**, 369-370.